Data Rate Fingerprinting: A WLAN-Based Indoor Positioning Technique for Passive Localization

Yaoxin Duan, Kam-Yiu Lam, *Member, IEEE*, Victor C. S. Lee, *Member, IEEE*, Wendi Nie, Kai Liu, *Member, IEEE*, Hao Li, and Chun Jason Xue, *Member, IEEE*

***Abstract*— Received signal strength (RSS)/channel state information (CSI) fingerprinting techniques have been widely adopted for wireless local area network (WLAN)-based indoor localization. However, in most of the RSS/CSI fingerprinting techniques, an application/software has to be installed on the target for uploading RSS/CSI information to the localization system. As a result, RSS/CSI fingerprinting cannot achieve passive localization (application-free), which is an essential requirement in many existing localization systems, especially for commercial and military purposes. In this paper, we propose *data rate (DR) fingerprinting* to achieve passive localization. DR fingerprinting is compatible with most off-the-shelf wireless fidelity (Wi-Fi) devices and can be directly implemented in the existing WLAN-based localization system without any extra hardware. In DR fingerprinting, DRs are used to replace the RSS/CSI to form fingerprints, since DR information can be directly obtained by access points (APs). However, the inherent features of DR, including low-resolution and serious fluctuation, significantly impair the performance of DR fingerprinting. For implementing DR fingerprinting, we leverage multiple transmission power levels, propose a time-window mechanism with different fingerprint formulations, design a AP switching strategy, and design a new matching algorithm named dynamic nearest neighbors (DNNs). We conducted extensive experiments in a real-world testbed to study the performance of DR fingerprinting. Specifically, we compared DR fingerprinting with the state-of-the-art RSS/CSI fingerprinting techniques. The experimental results illustrate that DR fingerprinting can achieve the localization accuracy that is comparable to that of the RSS/CSI fingerprinting with the additional benefit of achieving passive localization.**

***Index Terms*— WLAN-based localization, fingerprinting, passive localization, data rate.**

I. Introduction

WIRELESS local area network based indoor localization has attracted increasing research attention for years, as it can offer the basis for various novel mobile applications [1], [2] by utilizing widely deployed infrastructure of WLAN such as wireless fidelity (Wi-Fi) access points (APs) to build low-complexity and cost-effective indoor localization systems. Among various techniques proposed by previous works for WLAN-based indoor localization, the received signal strength (RSS)/Channel State Information (CSI) fingerprinting[1] [3]–[5] is one of the most promising techniques as it is effective in complex indoor environment. RSS fingerprinting uses RSS at different locations to build the fingerprints. Intuitively, the RSS could either (1) be scanned by APs, through detecting the signals sent by a Wi-Fi mobile client/target; or inversely, (2) be scanned by the target, through detecting the signals sent by APs. Since the target may adjust its transmission power to save energy or to enhance the signal quality [6], the RSS collected using method (1) is unstable. In order to collect stable RSS, most of the existing RSS fingerprinting techniques [7], [8] adopt method (2) to collect RSS by setting APs at a fixed transmission power. As a result, a specially designed application/software is required to be installed at the target for scanning and uploading the RSS to the system. However, this requirement renders RSS fingerprinting inapplicable for *passive localization*.

Passive localization is to locate a target without requiring any dedicated application/software (i.e., application-free) at the target to participate in the localization process [9], [10]. It is an essential requirement in many existing localization systems. First, it may not be practicable to require users of Wi-Fi clients to install the application, especially in commercial and military scenarios. Second, it may not be possible for some targets to have the application installed since their functionalities are either primitive or fixed (e.g., early mobile phone and body sensors).

In this paper, we propose a novel fingerprinting technique named *data rate (DR) fingerprinting* to achieve passive

[1]Hereafter, we use RSS fingerprinting to replace RSS/CSI fingerprinting.

Manuscript received February 22, 2019; revised April 9, 2019; accepted April 9, 2019. Date of publication April 17, 2019; date of current version July 3, 2019. This work was supported in part by the Fundamental Research Funds for the Central Universities under Project 2019CDXYZDH0014, in part by the City University Strategic under Grant 7004883, in part by the National Science Foundation of China under Grant 61572411, Grant 61872049, and Grant 61703066, in part by the Frontier Interdisciplinary Research Funds for the Central Universities under Project 2018CDQYJSJ0034, in part by the Natural Science Foundation Project of Chongqing under Grant cstc2018jcyjAX0536, and in part by the Chongqing Municipal Education Commission under Grant KJ1600402. The associate editor coordinating the review of this paper and approving it for publication was Prof. Huang Chen Lee. *(Corresponding author: Wendi Nie.)*

Y. Duan is with the Key Laboratory of Industrial Internet of Things and Networked Control, Ministry of Education, Chongqing University of Posts and Telecommunications, Chongqing 400065, China, and also with the College of Automation, Chongqing University of Posts and Telecommunications, Chonqing 400065, China (e-mail: iven0206@gmail.com).

K.-Y. Lam, V. C. S. Lee, and C. J. Xue are with the Computer Science Department, City University of Hong Kong, Hong Kong (e-mail: cskylam@cityu.edu.hk; csvlee@cityu.edu.hk; jasonxue@cityu.edu.hk).

W. Nie is with the College of Automation, Chongqing University, Chongqing 400030, China (e-mail: wendynie0325@gmail.com).

K. Liu is with the College of Computer Science, Chongqing University, Chongqing 400030, China (e-mail: liukai0807@cqu.edu.cn).

H. Li is with the Computer Science Department, Hong Kong Baptist University, Hong Kong (e-mail: cshaoli@comp.hkbu.edu.hk).

Digital Object Identifier 10.1109/JSEN.2019.2911690

localization. In DR fingerprinting, instead of using RSS, data rate information of packets transmitted from APs to the target is used for building the fingerprints. In summary, DR fingerprinting has the following advantages: (1) DR fingerprinting addresses the passive localization problem that RSS fingerprinting encountered; and (2) the applicability of DR fingerprinting is wide. DR fingerprinting can be directly implemented in existing WLAN-based localization systems without any extra hardware. It is compatible with the off-the-shelf Wi-Fi devices, as the mechanism of DR fingerprinting strictly follows WLAN protocols, e.g., 802.11a/b/g and 802.11n/ac, etc.

The design of DR fingerprinting is based on the following two observations. First, in WLAN-based localization systems, APs can support multiple data rates for transmitting packets to a target to adapt to different channel quality. Specifically, the data rates at different locations are different. Therefore, we can distinguish targets at different locations by observing their data rates. Second, the data rate of transmitting packets from an AP to a target can be obtained directly by the AP, which is stipulated in the IEEE standards of WLAN. Therefore, the target does not need to install any additional applications to obtain data rates.

Implementing DR fingerprinting faces three challenges as follows. First, the resolution of data rates of most existing Wi-Fi APs is low, which impairs the performance of DR fingerprinting, as a higher resolution usually results in a higher localization performance in terms of accuracy. For example, there are 8 levels of data rate for APs working in IEEE 802.11g standard, while RSS usually range from -20dBm to -95dBm, with 1dBm step. Second, similar to RSS, the data rate is not stable and may fluctuate in an indoor environment due to changing channel conditions. Third, in DR fingerprinting, to locate a target, the data rates of ALL APs are required. To collect the data rates of one AP, a target must associate with an AP in advance, then the AP is enabled to transmit packets to the target. However, once a target is associated with an AP, it would not actively switch to associate with another AP. Therefore, a mechanism is required for forcing the target to associate with each AP one by one to collect the data rates of all APs.

The following solutions are proposed to resolve the above problems. First, we leverage the multiple power levels of APs to enhance the resolution of data rates. The state-of-the-art APs are able to adjust their transmission power among several discrete levels (e.g., 30dBm, 20dBm, 10dBm, 0dBm, etc.) [6], [11], [12], which enables data rate at different power levels to form a new dimension of fingerprints. Second, we propose a time window mechanism to resolve the problem of fluctuating data rate. Based on the data rates of the target at a location collected within a time window, three different formulations of data rate fingerprints, named *the most frequent data rate (MFDR), the two most frequent data rates (TMFDR)* and *the full distribution of collected data rates (FDoDR)*, are proposed to build the fingerprint of the target for a better representation of the location. Third, we propose an AP switching strategy which enables the target to switch from its associated AP to another AP one by one, without any dedicated software installed on the target. In addition, to improve the performance of DR fingerprinting, we propose a tailor-designed matching algorithm named *dynamic nearest neighbor (DNN)* algorithm. DNN is an extension of the k-nearest neighbor (KNN) algorithm, which is a matching algorithm widely adopted in RSS fingerprinting [13]. Specifically, DNN dynamically selects the number of nearest neighbors according to different situations to improve accuracy.

In summary, this paper has the following main contributions:

- By leveraging data rate information, DR fingerprinting achieves passive localization. To the best of our knowledge, this is the first paper that addresses the passive localization problem encountered in RSS fingerprinting techniques.
- To implement DR fingerprinting, we leverage multiple power levels, study a time window mechanism together with three different fingerprint formulations, propose an AP switching strategy and design the DNN algorithm.
- We have conducted extensive experiments in a real-world testbed to study the performance of DR fingerprinting as compared with typical RSS fingerprinting techniques. The experimental results demonstrate that DR fingerprinting can achieve fine-grained accuracy (i.e., approximately 2-3 meters on average in terms of distance error) and its performance is comparable to that of the state-of-the-art RSS fingerprinting techniques.

The rest of this paper is organized as follows. Section II discusses related works. The system model of DR fingerprinting is introduced in Section III. Section IV first studies three challenges for implementing DR fingerprinting as well as their solutions. Then, the DNN algorithm is proposed to improve the performance of DR fingerprinting. Section V presents the settings of our experiments and reports the experimental results. Finally, we conclude the paper in Section VI. For readers' convenience, we summarize a set of symbols, notations, and abbreviations, which are frequently used in this paper, in Table I.

II. Related Work

A broad class of wireless localization techniques has been proposed for indoor environments, such as using RFID, ultra-wide band (UWB) measurements, WLAN and Bluetooth, etc. Among them, WLAN-based indoor localization reveals its benefits in better universality and efficiency, as WLAN infrastructures have already been widely deployed in hot areas such as shopping malls and government buildings for Internet accesses [14], [15].

In the past decade, a notable surge of commercial interests emerged using RSS fingerprinting techniques for WLAN-based indoor localization [16], due to that (1) it is easy to obtain RSS information at a Wi-Fi device by monitoring received packets; and (2) fingerprinting techniques do not require line-of-sight measurement, thereby it is suitable in complex indoor environments. Most of the previous works focused on the performance issues of using RSS fingerprinting, either on exploring the properties of RSS or combining with other information. Kaemarungsi and Krishnamurthy [17]

TABLE I
FREQUENTLY USED SYMBOLS, ABBREVIATIONS AND THEIR DEFINITIONS

Symbols and Abbreviations	Definitions
AoI	Area of interest
AP	Access point
AC	Access point controller
RP	Reference point
TP	Testing point
Target	A WiFi mobile client which is being located
RSS	Received signal strength
DR	Data rate
MFDR	The most frequent data rate
TMFDR	The two most frequent data rates
FDoDR	The full distribution of collected data rates
KNN	K nearest neighbors
DNN	Dynamic nearest neighbors
N	The number of pre-selected RPs
P	The number of pre-deployed APs
L	The number of transmission power levels
Z	The number of data rate levels
CDF	Cumulative distribution function

investigated the RSS data to understand the performance properties of the RSS fingzerprinting techniques. Feng *et al.* [18] proposed an accurate RSS-based positioning system with the use of the theory of compressive sensing. Chen *et al.* [19] proposed a sensor fusion framework running on a smartphone by combining RSS of Wi-Fi signals, pedestrian dead reckoning, and landmarks. However, most of existing RSS fingerprinting techniques require a dedicated software installed on targets to scan RSS and to upload collected RSS information to the localization system. Therefore, it is infeasible for passive localization.

Device-free passive (DFP) localization techniques [20] and triangulation technique [21] can achieve passive localization. DFP localization techniques are designed based on a fact that the human body is reacting as an absorber attenuating the wireless signal. In [20], long-term RSS records of the environment is compared with the short-term/current RSS records. A maximum likelihood estimator is adopted to process the compared RSS records to estimate the location of a target. However, DFP localization techniques are vulnerable to multi-subject interferences, and their ability to track multiple entities simultaneously with high accuracy is limited [22]. In triangulation techniques, taking [21] for example, APs monitor wireless channels to obtain RSS of wireless signals sent by a target. Then, the collected RSS is transformed into the distances between the APs and the target to calculate the location of the target. However, the transformation is based on a theoretical propagation model and line-of-sight (LoS), which are impractical in complex indoor environments. Comparing with DFP and triangulation, fingerprinting techniques are able to locate multiple objects in an indoor environment with high accuracy. Therefore, in this paper, we propose DR fingerprinting which can satisfy the requirement of passive localization while good performance is maintained for indoor localization.

III. SYSTEM MODEL OF DATA RATE FINGERPRINTING

A. System Architecture

Figure 1 depicts the system architecture of DR fingerprinting which consists of a number of APs, a wireless access point controller (AC), and a localization server. APs are pre-deployed at specific locations in the area of interest (AoI). The APs have two types of network interfaces. One is a wireless interface which can communicate with targets (e.g., mobile phones or laptops). The other is a wired interface which connects to the AC and the localization server. The AC is responsible for configuring and controlling the APs. The localization server maintains a fingerprint database which stores fingerprints of reference points (RPs) and is able to receive information collected by APs via wired connections. The details of RPs will be discussed in the later section. Based on the database and the information, the server estimates the location of the targets.

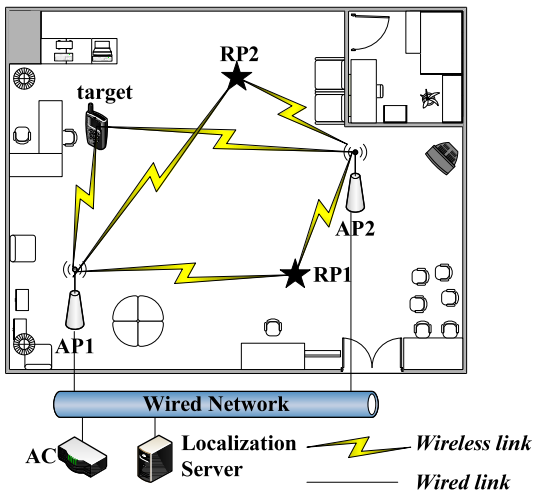

Fig. 1. The system architecture of DR fingerprinting.

B. Workflow

The workflow of DR fingerprinting consists of an offline phase and an online phase as shown in Figure 2.

1) Offline Phase: The offline phase performs a site survey of the AoI to build a fingerprint database. As depicted in Figure 2, first, some locations are selected as RPs, which are known and fixed locations within the AoI. Second, the coordinates of all RPs are collected and stored in the fingerprint database. For instance, it is assumed that there are N pre-selected RPs and P identical APs in the AoI. Third, a Wi-Fi device is deployed at each RP, and the APs send sample data packets to the Wi-Fi device. Fourth, each AP collects the data rates of the packets for each RP. The data rate of the packets, which is transmitted from the p^{th} AP to the i^{th} RP, is denoted by dr_p^i, where $p \in \{1, 2, \ldots, P\}$, $i \in \{1, 2, \ldots, N\}$ and $dr_p^i \in Z$. Z represents the set of data rate levels. For example, in 802.11g, there are 8 levels of data rates, which are level 1 (6Mbps), level 2 (9Mbps), level 3 (12Mbps), level 4 (18Mbps), level 5 (24Mbps), level 6 (36Mbps), level 7 (48Mbps) and level 8 (54Mbps). In the case, Z = {1,2, …, 8}. If the data rate of the packets transmitted from the p^{th} AP to the i^{th} RP is 12 Mbps, dr_p^i equals 3. Consequently, the data rate fingerprint (DR fingerprint) of the i^{th} RP is formulated as follows:

$$[dr_1^i, \ldots, dr_p^i, \ldots, dr_P^i], \tag{1}$$

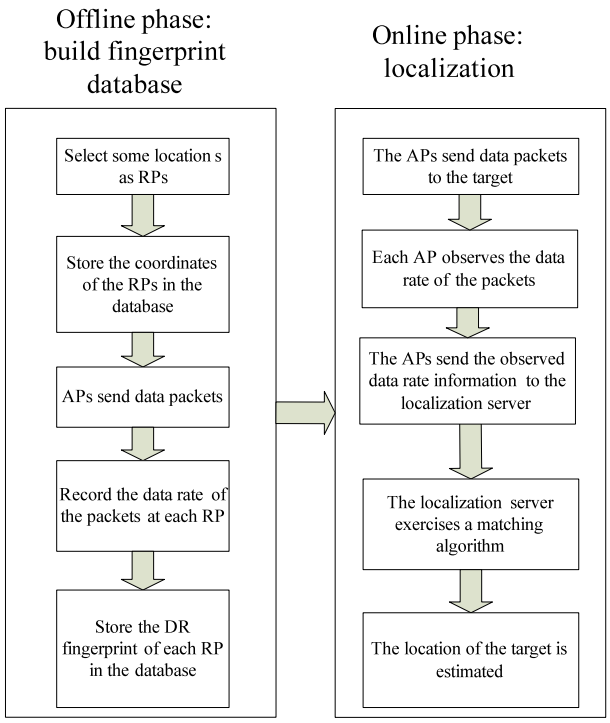

Fig. 2. The workflow of DR fingerprinting.

Finally, the DR fingerprints of all RPs are stored in the database, which could be used for location estimation in the online phase to be introduced in the following section.

2) Online Phase: In the online phase, the DR fingerprint of the target is collected and compared with the database to estimate the location of the target. The location of a target is referred to as a testing point (TP). As depicted in Figure 2, when the system is locating the target, first, the APs transmit data packets to the target. Second, the APs observe the data rates of the transmitted packets. Third, the APs send the observed data rate information to the localization server through the wired network. The observed data rates of all APs form the DR fingerprint of the TP as follows:

$$[dr_1^{TP}, \ldots, dr_p^{TP}, \ldots, dr_P^{TP}], \tag{2}$$

where dr_p^{TP} is the observed data rate of the packets which are transmitted from the p^{th} AP to the target and $dr_p^{TP} \in Z$. Fourth, the localization server exercises a matching algorithm to estimate the coordinates of the TP based on the DR fingerprint of the TP and the DR fingerprint database built in the offline phase. Specifically, the matching algorithm estimates the coordinates of the target by computing the similarity between the fingerprint of the TP and the fingerprint of each RP.

It can be observed that during the localization process of DR fingerprinting in the online phase, the target is free from installing any dedicated software to upload any information to the localization server. Therefore, DR fingerprinting achieves passive localization. However, due to the inherent features of data rate, implementing DR fingerprinting faces challenges, which will be introduced in the following section.

IV. Challenges and Solutions for Implementing DR Fingerprinting

In this section, first, we introduce three challenges for implementing DR fingerprinting, and then we propose their solutions. The challenges are low resolution of data rate, fluctuating data rate, and the AP switching problem. Second, to improve the performance of DR fingerprinting, we propose the DNN algorithm which is able to dynamically select the number of nearest neighbors of TPs.

A. Low Resolution of Data Rate

DR fingerprinting faces the challenge of low resolution of data rate, as a low resolution usually results in a low localization performance in terms of accuracy. Specifically, an AP has relatively limited levels of data rates for transmitting packets (e.g., eight levels in IEEE 802.11g standard), while RSS generally has dozens of levels. As a result, the AoI is divided into sparse areas of data rates, which impairs the performance of DR fingerprinting.

To enhance the resolution of data rate, we leverage the adjustable transmission power of the off-the-shelf APs. Generally, for a target at a specific location, adjusting the transmission power of an AP can change the data rate used by the AP for transmitting packets to the target. Multiple power levels introduce a new dimension to build the data rate fingerprints, and thereby increases the resolution of data rate such that the AoI can be separated into more areas in the signal space.

Figure 3 is an example to demonstrate how multiple power levels increase the resolution of data rates, and thus improving the localization accuracy of DR fingerprinting. It is assumed that the APs in Figure 3(a) support two data rates (named, high rate and low rate), and have one transmission power level. In particular, the APs use high rate to send data packets to the target if it is within the dashed circle, while the APs use low rate if the target is within the ring between the dashed circle and solid circle. The target in Figure 3(a) is estimated within the shaded area as the data rate is high and zero (out of transmission range), corresponding to AP1 and AP2, respectively. Obviously, the accuracy is poor as the shaded area is large. In Figure 3(b), AP2 has two transmission power levels. Therefore, the numbers of dash circles and solid circles increase accordingly. Combining the data rate information observed from both AP1 and AP2 for all power levels, the target's location is then estimated to be within the shaded area as shown in Figure 3(b), and the accuracy is better as the shaded area is smaller than that in Figure 3(a).

To implement multiple transmission power levels in DR fingerprinting, DR fingerprints of RPs in the offline phase and DR fingerprints of TPs in the online phase have to be reformulated. In the offline phase, DR fingerprinting collects the data rate information at all transmission power levels of each AP. For instance, an AP adjusts its transmission power to transmit sample data packets to each RP at each power level. It is assumed that there are L levels of transmission power for each AP. If the p^{th} AP is operating at the l^{th} power level, the data rate of the packets, which is transmitted from the AP to the i^{th} RP, is denoted by $dr_{l,p}^{i}$,

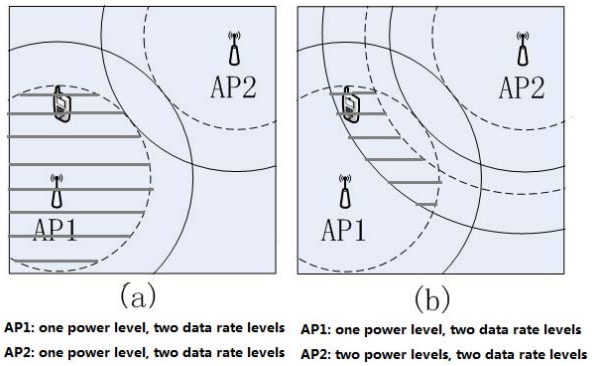

Fig. 3. An example to demonstrate how multiple power levels increase the resolution of data rate: (a) using one power level and (b) using two power levels.

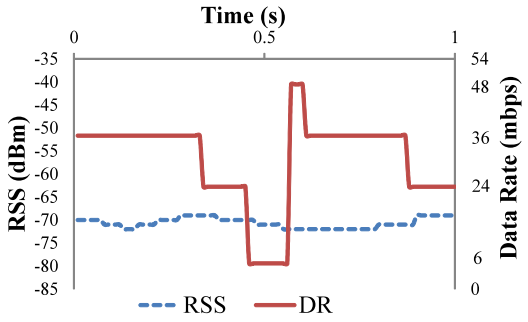

Fig. 4. An example that compares the fluctuation of RSS with that of data rate in one second.

where $l \in \{1, 2, \ldots, L\}$. Consequently, the DR fingerprint of the i^{th} RP can be formulated as follows:

$$\begin{bmatrix} dr^i_{1,1} & \cdots & dr^i_{1,p} & \cdots & dr^i_{1,P} \\ \vdots & \ddots & \ddots & \ddots & \vdots \\ dr^i_{l,1} & \ddots & dr^i_{l,p} & \ddots & dr^i_{l,P} \\ \vdots & \ddots & \ddots & \ddots & \vdots \\ dr^i_{L,1} & \cdots & dr^i_{L,p} & \cdots & dr^i_{L,P} \end{bmatrix}, \tag{3}$$

where $dr^i_{l,p}$ denotes the data rate of the packets transmitted from the p^{th} AP to the i^{th} RP while the AP is operating at the l^{th} power level and $dr^i_{l,p} \in Z$.

In the online phase, similarly, the DR fingerprint of a TP is formulated as follows:

$$\begin{bmatrix} dr^{TP}_{1,1} & \cdots & dr^{TP}_{1,p} & \cdots & dr^{TP}_{1,P} \\ \vdots & \ddots & \ddots & \ddots & \vdots \\ dr^{TP}_{l,1} & \ddots & dr^{TP}_{l,p} & \ddots & dr^{TP}_{l,P} \\ \vdots & \ddots & \ddots & \ddots & \vdots \\ dr^{TP}_{L,1} & \cdots & dr^{TP}_{L,p} & \cdots & dr^{TP}_{L,P} \end{bmatrix}, \tag{4}$$

where $dr^{TP}_{l,p}$ represents the observed data rate of the packets which are transmitted from the p^{th} AP to the target while the AP is operating at the l^{th} power level and $dr^{TP}_{l,p} \in Z$.

B. Fluctuating Data Rate

DR fingerprinting faces another challenge that data rate is not stable and may fluctuate significantly even though the location of a target does not change. In other words, there could be a big difference between the data rates at different times. The fluctuation of data rate is due to changing channel conditions, which are affected by a number of environmental factors, including shadow fading, multipath propagation, and interferences, etc. Determining the data rate among the fluctuating data rates to form DR fingerprints of TPs is a challenging problem since the location estimation should be finished in a short period of time in the online phase. In the offline phase, forming DR fingerprints of RPs is less affected by fluctuating data rates, since there is no time limit to collect data rates and a representative and relatively stable data rate can be obtained.

To explain the fluctuating data rate problem, we give a simple example in Figure 4. In the example, an AP transmits 100 packets in 1 second to a target at a fixed location (i.e., a TP). The AP supports 12 levels of data rates. It is observed that compared with RSS, data rates fluctuate seriously. The lowest data rate (i.e., 6 Mbps) is close to the minimum data rate (i.e., 1 Mbps), while the highest data rate (i.e., 48 Mbps) is close to the maximum data rate (i.e., 54 Mbps).

To resolve the problem, we adopt a time window mechanism, which uses the data rates of packets in a period of time to determine an appropriate data rate. In the time window mechanism, three formulations of DR fingerprints of TPs are proposed, named the most frequent data rate (MFDR), the two most frequent data rates (TMFDR) and the full distribution of collected data rates (FDoDR).

In MFDR, the most frequent data rate among the packets collected in a time window is chosen to form the DR fingerprint of the TP. The rationale of MFDR is that, as can be observed in Figure 4, 36 Mbps is the most frequent data rate (More than half of the packets are transmitted using 36 Mbps.). Therefore, 36 Mbps is selected as an appropriate data rate to form the DR fingerprint of the TP.

In TMFDR, the two most frequent data rates among the packets collected in a time window are combined to form the DR fingerprint of the TP. For example, in Figure 4, the two most frequent data rates (i.e., 36 Mbps and 24 Mbps) cover more than 80% of the packets. Let $dr1$ and $dr2$ denote the two most frequent data rates in a time window. It is assumed that there are $M1$ packets using the data rate of $dr1$ during the time window, while there are $M2$ packets using the data rate of $dr2$ during the time window. Therefore, in TMFDR, the DR fingerprint of the TP is built as follows:

$$dr^{TP}_{l,p} = [(dr1, M1), (dr2, M2)]. \tag{5}$$

In FDoDR, all data rates among the packets collected in a time window are combined to form the DR fingerprint of the TP. It is assumed that there are M packets in the time window. The data rate of the m^{th} packet is denoted by s_m. The DR fingerprint of the TP is built as follows:

$$dr^{TP}_{l,p} = [s_1, s_2, \ldots, s_M]. \tag{6}$$

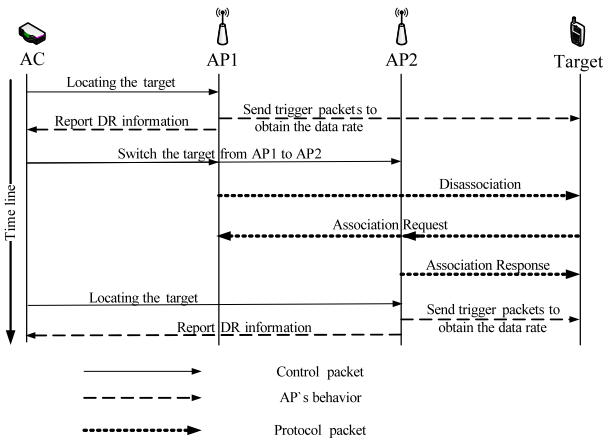

Fig. 5. The procedure of AP switching strategy.

C. AP Switching

The last challenge for implementing DR fingerprinting is the AP switching problem. In the online phase, a target must associate with every AP to receive data packets, as the data rates of ALL APs are required to form the DR fingerprint. However, once a target associated with an AP, it would not actively switch to another AP. Therefore, we propose an AP switching strategy which enables the target to switch from its currently associated AP to another AP one by one, without any dedicated software installed on the target. The AP switching strategy strictly follows the standards of the inter-AP handover and roaming in 802.11 networks [23], therefore, it is compatible with off-the-shelf Wi-Fi devices.

Figure 5 illustrates the working process of the AP switching strategy. All APs are covered by an extended service set (ESS), in other words, the APs have the same service set identifier (SSID). Initially, it is assumed that a target is associated with AP1. When locating the target, AP1 sends trigger packets to the target. Then, AP1 observes the data rate of the packets and reports the data rates to the AC. Subsequently, the AC forces AP1 to actively disassociate with the target. Following the WLAN protocol, the target automatically tries to associate with an AP having the same SSID by broadcasting an association request. Then, the AC asks AP2 to respond to the request for making the target associated with AP2. Similar to AP1, data rates observed by AP2 is then reported to the AC. The AP switching strategy repeats the above steps to make the target associated with remaining APs one by one. It is observed that the switching process is controlled by the AC and follows WLAN standards, and therefore, no extra hardware or dedicated application is required on targets.

D. Effect of AP Switching and Changing Power

In DR fingerprinting, it is notable that when a target is under localization, during the process of AP switching, the target would be affected, as it should switch to associate with the APs one by one. The switching process can take considerable time (up to seconds) for re-establishing connectivity to a new AP. The time for re-establishing connectivity would certainly impair users' experience, as they may lose network connectivity for seconds. Therefore, it is a challenging problem to support real-time localization in DR fingerprinting. A lot of previous works have put efforts in providing fast handover for 802.11 WLAN [24], [25]. Their works have significantly reduced the handover time, and thus is able to provide seamless AP switching. In this paper, we focus on the feasibility of DR fingerprinting and the localization performance of DR fingerprinting, rather than the real-time performance. We leave the problem of providing high-quality real-time localization services in DR fingerprinting as an important future work.

Changing APs' transmission power would also impair users' experience. For instance, when an AP decreases its transmission power, the data rate of the targets would be reduced. More seriously, the targets at the margin of the AP's signal coverage may lose network connectivity.

It is notable that, for IEEE 802.11n/ac standards, the MIMO-based beamforming [26] function would affect the implementation of DR fingerprinting, as the data rate of a particular target not only depends on the position of the user, but also depends on the number and positions of the devices associated with the same AP of the target. Therefore, the APs which works in 802.11n/ac model must turn off the beamforming function when performing localization using DR fingerprinting.

E. The Dynamic Nearest Neighbor Algorithm

To improve the performance of DR fingerprinting, we propose a tailor-designed matching algorithm named dynamic nearest neighbor (DNN) algorithm. Recall that in the online phase, a matching algorithm is exercised to estimate the coordinates of targets. The k-nearest neighbor (KNN) algorithm [27] is a popular matching algorithm adopted by most of the RSS fingerprinting techniques.

The performance of KNN is highly affected by the predetermined crucial parameter k (i.e., the number of nearest neighbors). For example, in Figure 6, the estimated locations of target 1 and target 2 using the KNN algorithm with different values of k are illustrated. For simplification, in Figure 6, we assume that the difference in signal space between two locations is exactly the same as the Euclidean distance between them. If $k = 2$, the KNN algorithm estimates that target 1 and target 2 are located in the midpoint of RPs A and B, and the midpoint of RPs D and E, respectively. However, if $k = 3$, the KNN algorithm estimates that target 1 and target 2 are located at the centroid of the triangle ABC and the centroid of the triangle DEG, respectively. Obviously, neither $k = 2$ nor $k = 3$ of the KNN algorithm can estimate the most accurate locations for *both* target 1 and target 2 at the same time.

To select an appropriate number of nearest neighbors for different targets, we propose DNN which is an extension of KNN. The basic principle of DNN is that DNN is able to *dynamically* select the number of nearest neighbors for different situations, rather than using a fixed number of neighbors in KNN. DNN adopts similarity in the signal space (i.e., the Euclidean distance) to calculate the difference between each RP and TP. To dynamically select the number of nearest neighbors of the TP, DNN sets a threshold, and the value of

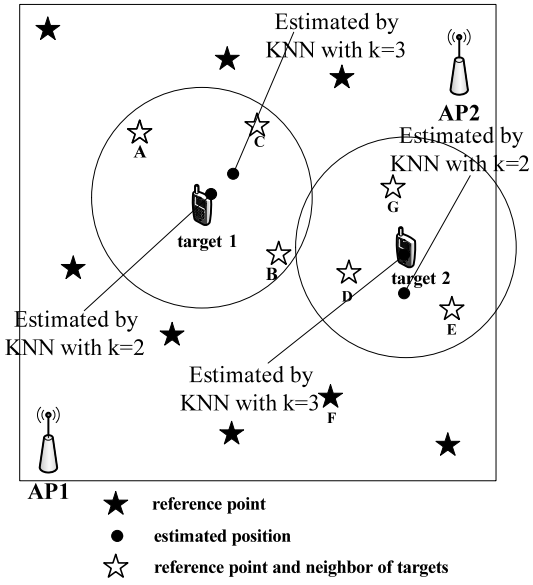

Fig. 6. An example to illustrate the limitation of using a fixed value of k in KNN: using KNN with k=2 is the best for target 1, while using KNN with k=3 is the best for target 2.

Algorithm 1 DNN algorithm

Input: P, N, $dr^i_{l,p}$, $< x^i, y^i >$, $dr^{TP}_{l,p}$
Output: $< x^{TP}, y^{TP} >$

1: $\tau \leftarrow 0$
2: **repeat**
3: **for** each $i \in [1, N]$ **do**
4: **for** each $p \in [1, P]$ **do**
5: $DiS^i_p \leftarrow \sum^l_{[1,L]} |dr^i_{l,p} - dr^{TP}_{l,p}|$.
6: **if** $DiS^i_p \leq \tau$ **then**
7: Let $i \in Nr_p$
8: **end if**
9: **end for**
10: **end for**
11: $NR \leftarrow Nr_1 \bigcap Nr_2 \bigcap ... \bigcap Nr_P$.
12: $\tau \leftarrow \tau + 1$
13: **until** NR is not empty
14: **for** each neighbor $j \in NR$ **do**
15: $DiSS^j \leftarrow \sqrt{\sum^p_{[1,P]} (DiS^j_p)^2}$.
16: **end for**
17: x^{TP} or $y^{TP} \leftarrow \sum^j_M (\frac{1/DiSS^j}{\sum^j_M (1/DiSS^j)} \times x^j$ or $y^j)$.

the threshold is automatically adjusted according to different situations. In particular, if the difference between the DR fingerprint of an RP and that of the TP does not exceed the threshold, the RP is selected as a neighbor of the TP.

The detailed steps of the DNN algorithm are given in Algorithm 1. The inputs of DNN are the number of APs (denoted by P), the number of RPs (denoted by N), the DR fingerprint of each RP (denoted by $dr^i_{l,p}$), the coordinates of each RP (denoted by $< x^i, y^i >$) and the DR fingerprint of the TP (denoted by $dr^{TP}_{l,p}$). The output of DNN is the estimated coordinates of the TP (denoted by $< x^{TP}, y^{TP} >$).

In line 1, the threshold, denoted by τ, is initialized to zero. From line 2 to line 13, DNN tries to obtain a neighbor set (non-empty) of the TP for all APs. First, from line 3 to line 5, DNN calculates the difference in signal space between RPs and the TP for *each* AP. Let DiS^i_p denote the difference between the i^{th} RPs and the TP for the p^{th} AP, where DiS^i_p is calculated by $\sum^l_{[1,L]} |dr^i_{l,p} - dr^{TP}_{l,p}|$. Each AP has a neighbor set of the TP. Let Nr_p denote the neighbor set of the TP for the p^{th} AP. Second, in line 6, DiS^i_p is compared with the threshold. If DiS^i_p is not larger than the threshold, the i^{th} RP is selected as a neighbor of the TP for the p^{th} AP, and the i^{th} RP is included in Nr_p in line 7. Third, in line 11, the intersection between the neighbor sets of all APs is obtained to represent the neighbor set of the TP for all APs, denoted by *NR*. From line 12 to line 13, if *NR* is empty, DNN increases the threshold by 1 and then repeats the above three steps until a non-empty *NR* is obtained. Here, "1" is the smallest unit of the difference between the RPs and the TP in signal space. Therefore, the value of τ depends on when *NR* is obtained.

From line 14 to line 16, DNN calculates the difference in signal space (DiSS) between the TP and each neighbor in *NR*. Let $DiSS^j$ denote the difference between the TP and the j^{th} neighbor in *NR*, where $j \in \{1, 2, \ldots, M\}$ and M is the number of neighbors in *NR*.

Finally, in line 17, the coordinates of the TP are estimated by averaging the weighted coordinates of the neighbors in *NR*. In particular, each neighbor is assigned a weight to its coordinates according to its DiSS. Let w^j denote the weight assigned to the coordinates of the j^{th} neighbor in *NR*, which is calculated by:

$$w_j = \frac{1/DiSS^j}{\sum^j_{1,M} (1/DiSS^j)}, \tag{7}$$

By averaging the weighted coordinates of the K neighbors, the coordinates of the TP are calculated by:

$$x^{TP}(or\ y^{TP}) = \sum^j_{1,K} (w^j \times x^j (or\ y^j)). \tag{8}$$

Figure 7 is an example to demonstrate the DNN algorithm. As shown in Figure 7, the target is located near the middle of A and B. When $\tau = 0$, after calculating DiS for each AP, we can find that Nr_1 has F and Nr_2 is empty. Therefore, *NR* is empty and then τ is increased by 1. After calculating DiS for each AP, we can find that Nr_1 has A, B, and F, while Nr_2 has A, B, D, and E. The intersection of the two neighbor sets is A and B, which are marked as hollow stars in Figure 7. Therefore, the set {A,B} is considered as the nearest neighbor set of the target. For simplification, we assume that the weights assigned to A and B are the same. Therefore, the DNN algorithm estimates that the target is located in the middle of A and B.

V. Performance Evaluation

A. Testbed and Settings

To study the feasibility and effectiveness of the proposed DR fingerprinting technique, we have conducted extensive experiments in a practical testbed. We deployed a number of

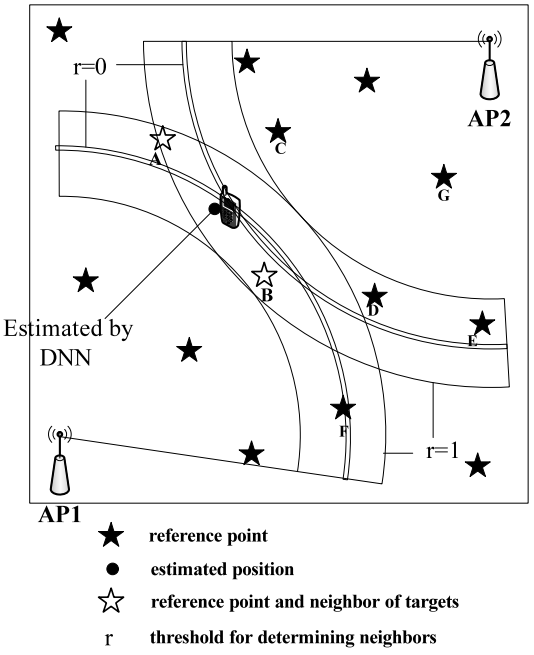

Fig. 7. An example of the DNN algorithm to determine neighbors: no neighbor when $\tau = 0$; two neighbors when $\tau = 1$.

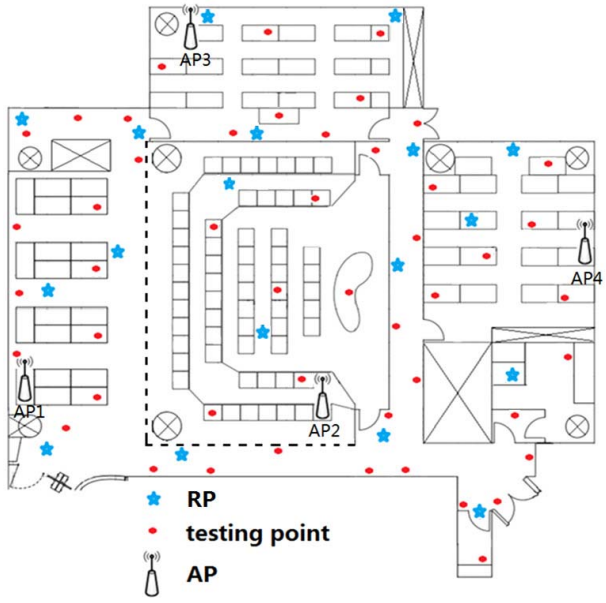

Fig. 8. The testbed of our experiments: a floor with isolated rooms, 25 meters by 25 meters; 4 APs; 18 RPs; 47 TPs.

COMPEX APs in the testbed and used a set of mobile devices including mobile phones and laptops as targets. The APs work on the operating system of OpenWrt 17.01.4 [28], while the Wi-Fi chipset is Qualcomm Atheros QCA9558.

Figure 8 depicts the deployment of the testbed (i.e., AoI). It is located on the second floor of MMW building at City University of Hong Kong, a 25 meters by 25 meters area. The noise floor of the environment is -92 dBm. We deployed 4 APs in the AoI, marked as black antennas. 18 locations were chosen as RPs, and they are marked as blue stars. The

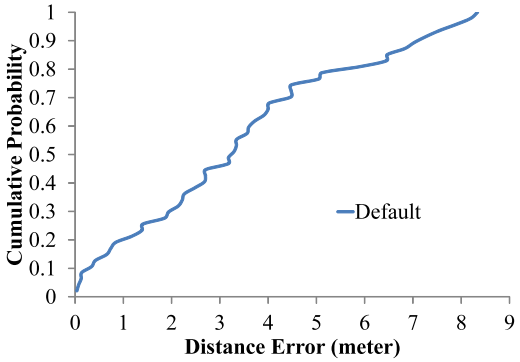

Fig. 9. CDF of distance error using the default settings.

average distance between two RPs is 5.9 meters. 47 TPs are selected and marked as red points. All RPs and TPs were randomly selected and were evenly distributed. 802.11b/g standard which has 12 levels of data rates is used as it is compatible with most existing Wi-Fi devices. For building the fingerprint database in the offline phase, we deployed a smartphone (Samsung G5308W) at each RP. Then, we collected data rate and RSS of all RPs separately in 15 different days. In total, about 1,000 mins of data rate/RSS traces were collected. In the online phase, we repeated 30 times (2 times per day) on different days to estimate the location of each TP.

In our experiments, we first defined default settings, and then changed the setting to study the impact of different settings on the performance of DR fingerprinting. The following lists the settings that we have studied, where the default settings are highlighted: (1) **number of APs**: 2, 3, 4 *(default)*; (2) **matching algorithm**: KNN, DNN *(default)*; (3) **fingerprint formulation**: MFDR *(default)*, TMFDR, FDoDR; (4) **transmission power of APs**: 0 dBm, 10 dBm, 20 dBm, 30 dBm, multiple power levels *(default)* including 0 dBm, 10 dBm, 20 dBm and 30 dBm; (5) **the size of time window**: 10s, 20s, 30s *(default)*, 60s; (6) **target device**: mobile phones including iPhone 6s Plus, Samsung G5308W *(default)*, Huawei MY1-AL10, laptops including MacBook Air, ACER 4752G.

In the following, the localization accuracy of each setting is illustrated in terms of the cumulative probability of distance error, where the distance error is the Euclidean distance between the estimated location and the actual location. The cumulative probability (i.e., cumulative distribution function (CDF)) refers to the probability that the value of distance error falls within a specified range of distances.

B. Experimental Results of Default Settings

In this section, we study the results of DR fingerprinting using the default settings. The localization accuracy of using the default settings is illustrated in Figure 9. The average distance error is 3.47 meters, and the precision is 50% within 3.18 meters and 80% within 5.11 meters.

Figure 10 presents the estimated location of each TP. In the figure, each estimated location and the actual location of the corresponding TP is connected by a straight line.

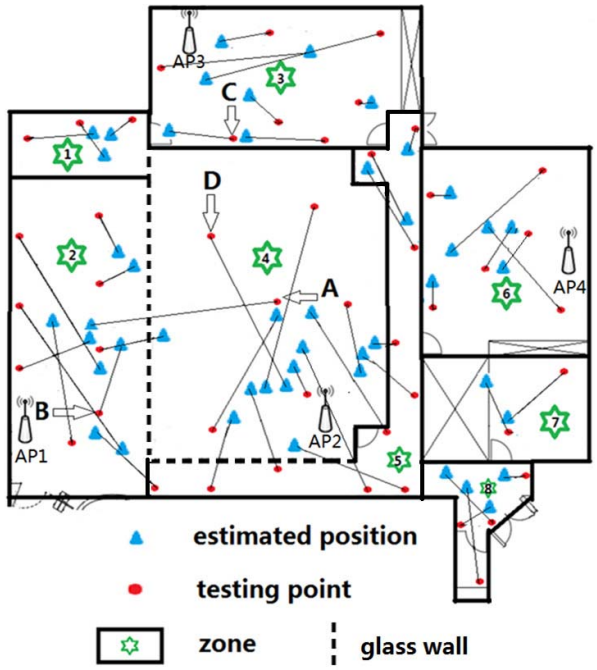

Fig. 10. The testbed is divided into 8 zones. The estimated location of each TP is linked to the TP.

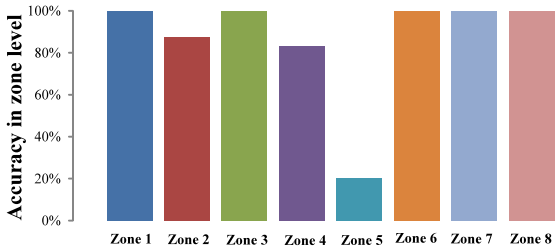

Fig. 11. The ratio of estimating correct zone for the TPs in each zone.

Considering that the channel condition in different rooms may be different, according to the room partition, we divide the entire testbed into several zones represented by bold lines (concrete partitions) or dash lines (glass wall). The percentage of estimating a correct zone for all TPs in each zone is shown in Figure 11. We observe that except zone 5, most of the estimated locations are in the same zone of the TPs. For instance, in Figure 10, although the distance error of TP D is large (i.e., 7.27 meters), both the estimated location and the TP are in the same zone (i.e., zone 4).

However, the estimated locations of some TPs are not in the same zone as the actual location of the TPs. We name this inconsistency as zone error. Most of the zone errors occur in zone 5, while other zone errors occur at the boundaries of zone 2 and zone 4. By analyzing the experimental data and the testbed environment, we figure out that zone errors are mainly due to the following two reasons. First, zone 5 includes two corridors which span a long and diverse area with no geometrical consistency to the other zones. If we divide zone 5 into two different zones (i.e., one horizontal and one vertical), the ratio of correct estimation in the vertical zone could be increased.

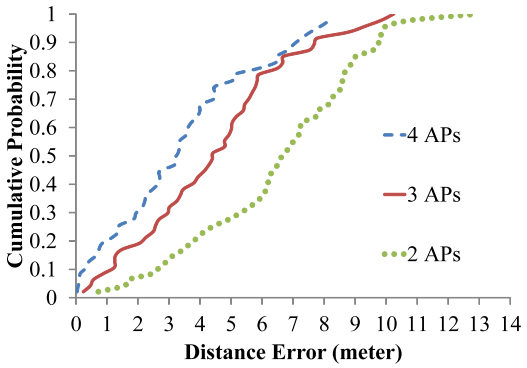

Fig. 12. CDF of distance error using different number of APs: 2 APs vs. 3 APs vs. 4 APs".

Furthermore, since the corridors are narrow, the TPs in zone 5 are close to the boundaries. Therefore, a small distance error may lead to zone errors. Second, the physical property of the zone partition leads to zone errors. We can observe from Figure 10 that almost all zone errors are close to the boundaries at the left side and the under side of zone 4. This is because the walls of the classroom in the middle, which are indicated by the dash lines in Figure 10, are made of glass rather than concrete. It is known that the propagation of wireless signal is significantly impaired by concrete, whereas glass does not impair the signal so much. Therefore, the division of zone 4 is debatable.

In summary, the localization results depict that DR fingerprinting can provide high accuracy for locating the target in zone level.

C. Effects of Different Parameter Settings

First, we study the impact of the number of APs on the performance of DR fingerprinting. Specifically, we exercised the 4 APs, all combinations of 3 APs over the 4 APs, and all combinations of 2 APs over the 4 APs. The results are presented in Figure 12. It can be observed that the distance error decreases with an increase in number of APs, where the average distance errors are 3.47 meters, 4.49 meters, and 6.56 meters, using 4 APs, 3 APs, and 2 AP2, respectively. In particular, the precision of using 4 APs is 50% within 3.18 meters and 80% within 5.11 meters. The precision of using 3 APs is 50% within 4.39 meters and 80% within 5.89 meters. The precision of using 2 APs is 50% within 6.58 meters and 80% within 8.61 meters. Basically, the results conform to previous works that the accuracy of fingerprinting technique is increasing with the number APs. If more APs are used, the accuracy will be higher.

Second, we study the improvement of using DNN by comparing DNN with KNN. For fairness, we exercised all possible values of k (i.e., $k \in \{1, 2, \ldots, N\}$) and used the best result of KNN for comparison. As shown in Figure 13, DNN outperforms KNN in most cases. The average distance errors are 3.47 meters and 4.26 meters, for DNN and KNN, respectively. In particular, the precision of DNN is 50% within around 3.18 meters and 80% within 5.11 meters, while the precision of KNN is 50% within 4.03 meters and 80%

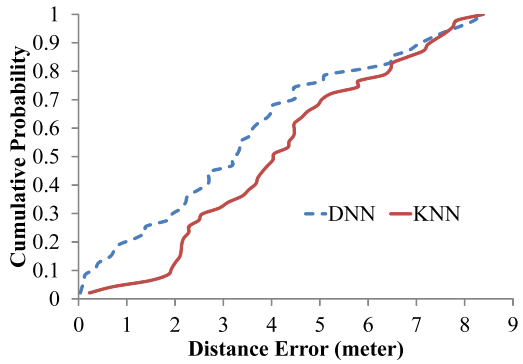

Fig. 13. CDF of distance error using different matching algorithms: DNN vs. KNN.

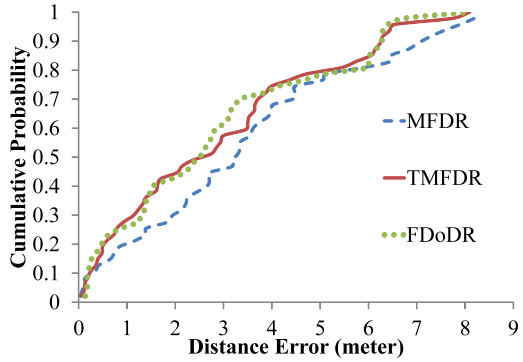

Fig. 14. CDF of distance error using different fingerprint formulation: MFDR vs. TMFDR vs. FDoDR.

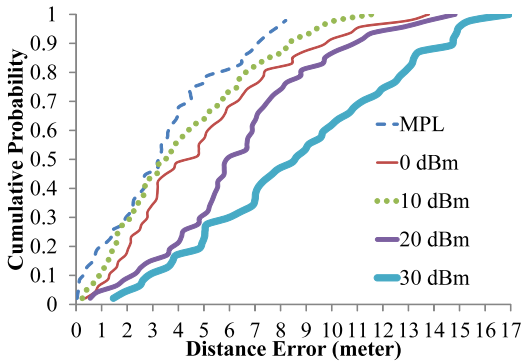

Fig. 15. CDF of distance error using different transmission power: using multiple power levels (denoted as MPL) vs. using fixed power levels (0 dBm, 10 dBm, 20 dBm, 30 dBm).

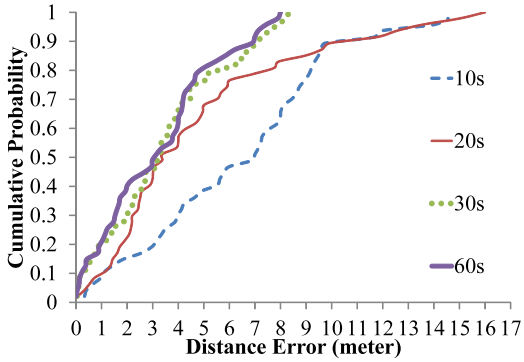

Fig. 16. CDF of distance error using different sizes of the time window: 10 s vs. 20 s vs. 30 s vs. 60s.

within 6.32 meters. The improvement achieved by DNN is approximately 0.8 meter. The experimental results demonstrate that DNN can efficiently improve the performance of DR fingerprinting.

Third, we study the performance of DR fingerprinting using three formulations of DR fingerprints (i.e., MFDR, TMFDR, FDoDR) in Figure 14. The average distance errors are 3.47 meters, 2.91 meters and 2.85 meters using MFDR, TMFDR, and FDoDR, respectively. In particular, the precision of MFDR is 50% within 3.18 meters and 80% within 5.11 meters. The precision of TMFDR is 50% within 2.36 meters and 80% within 4.73 meters. The precision of FDoDR is 50% within around 2.41 meters and 80% within around 5.09 meters. The performance of TMFDR and that of FDoDR are close to each other (0.06-meter difference). TMFDR and FDoDR outperform MFDR with an improvement of more than 0.5 meters. The reason is that the most frequent data rate used by MFDR only covers 50% to 60% of sample packets, while the two most frequent data rates used by TMFDR and the data rates used in FDoDR cover more than 80% of sample packets and 100% of sample packets, respectively.

Fourth, we study the performance of DR fingerprinting by leveraging multiple power levels, compared with fixed power levels in Figure 15. The distance errors using fixed power levels of 0 dBm, 10 dBm, 20 dBm, and 30 dBm are 5.03 meters, 4.23 meters, 6.52 meters, 8.76 meters on average, respectively, while the distance error using multiple power levels (denoted as MPL) is 3.47 meters on average. Particularly, the precision of MPL is 50% within 3.18 meters and 80% within 5.11 meters. The precision of 0 dBm is 50% within 3.95 meters and 80% within 7.33 meters. The precision of 10 dBm is 50% within 3.27 meters and 80% within 6.45 meters. The precision of 20 dBm is 50% within 5.81 meters and 80% within 8.77 meters. The precision of 30 dBm is 50% within 8.44 meters and 80% within 12.67 meters. The results demonstrate that, as discussed in Section IV-A, using multiple power levels can greatly improve the performance of DR fingerprinting, as the resolution of data rates is increased.

Fifth, we study the performance of DR fingerprinting using different sizes of the time window in Figure 16. The average distance errors using the window sizes of 10s, 20s, 30s, and 60s are 6.33 meters, 4.83 meters, 3.47 meters and 3.25 meters, respectively. In particular, the precision of 10 seconds as the window size is 50% within 6.88 meters and 80% within 9.11 meters. The precision of 20 seconds as the window size is 50% within 3.37 meters and 80% within 6.92 meters. The precision of 30 seconds as the window size is 50% within 3.18 meters and 80% within 5.11 meters. The precision of 60 seconds as the window size is 50% within 2.98 meters and 80% within 4.69 meters. It is observed that the performance using 10s and 20s are poor while those

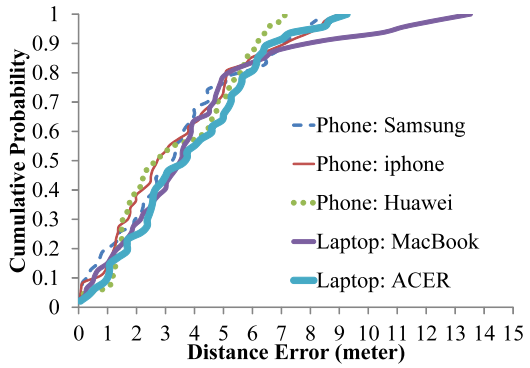

Fig. 17. CDF of distance error using different mobiles as targets: Phones (Samsung, iPhone, Huawei) vs. Laptops (MacBook, ACER).

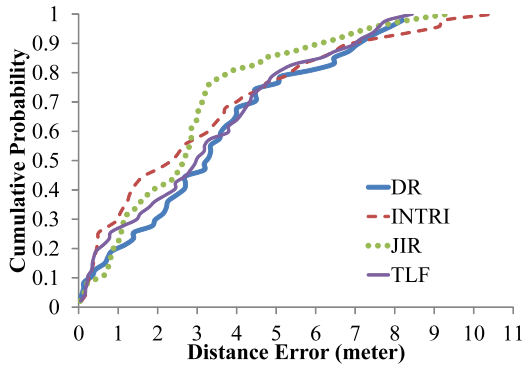

Fig. 18. CDF of distance error using different fingerprinting technique: DR vs. RSS (TLF, INTRI, JIR).

using 30s and 60s are relatively good because a larger size of the time window is better for collecting sufficient data rates to reflect the environmental condition of targets. The performance of using 30s and 60s are close to each other, which represents that using 30s as the window size is sufficient to achieve good performance. The reason is that a long size of time window requires the target to keep staying at a position for a long period of time, resulting in a poor performance in terms of real-time.

Finally, we study the performance of DR fingerprinting using different mobile devices as targets in Figure 17. It can be observed that the performance of using different mobile phones is similar. Specifically, the distance errors using Samsung, iPhone, and Huawei are 3.47 meters, 3.43 meters, and 3.38 meters, respectively. The performance of using laptops is slightly worse than using mobile phones. Specifically, the average distance errors using MacBook and ACER are 4.01 meters and 3.89 meters, respectively. This is because the fingerprint database was built using Samsung. The results demonstrate that different types of mobile devices do not significantly affect the performance of DR fingerprinting.

D. Comparing With RSS Fingerprinting

Previous works [29] have shown that the average distance error of RSS fingerprinting techniques is generally around 3-5 meters. From the discussions in the sections above, we can conclude that DR fingerprinting provides a competitive performance with RSS fingerprinting. To further demonstrate the conclusion, we compared DR fingerprinting with state-of-the-art RSS fingerprinting techniques, which are **TLF** [16], **INTRI** [30], and **JIR** [31] in Figure 18, where DR represents the results using DR fingerprinting.

The average distance error of DR fingerprinting is 3.47 meters, which is slightly worse than those of TLF, INTRI, and JIR, which are 3.24 meters, 3.09 meters, and 2.83 meters, respectively. In particular, the precision of DR is 50% within 3.18 meters and 80% within 5.11 meters. The precision of TLF is 50% within 2.94 meters and 80% within 4.89 meters. The precision of INTRI is 50% within 2.24 meters and 80% within 5.21 meters. The precision of JIR is 50% within 2.63 meters and 80% within 3.63 meters. To sum up, the experimental results conform to our belief that although DR fingerprinting may not perform as good as RSS fingerprinting, it can provide acceptable localization performance with the additional benefit of being able to locate the targets passively.

VI. Conclusion

In this paper, we propose a novel fingerprinting, named DR fingerprinting, for passive localization. This is the first paper addressing passive localization of RSS fingerprinting. In particular, DR fingerprinting leverages data rates, which can be directly obtained by the localization system, to form the fingerprints of the RPs and the TPs. The experimental results show that the localization accuracy of DR fingerprinting can achieve good performance comparable to that of RSS fingerprinting.

Nevertheless, there are other methods to improve DR fingerprinting. For example, an important future work is to improve the real-time performance of DR fingerprinting, as the AP switching strategy may take considerable time to re-establishing connectivity. Moreover, since the localization accuracy of fingerprinting techniques is highly related to the distribution of RPs, another important future work of DR fingerprinting is to optimizing the distribution of reference points. Another interesting future work is to adapt DR fingerprinting in MIMO-based beamforming system of 802.11n/ac.

References

[1] S.-H. Fang, W.-H. Chang, Y. Tsao, H.-C. Shih, and C. Wang, "Channel state reconstruction using multilevel discrete wavelet transform for improved fingerprinting-based indoor localization," *IEEE Sensors J.*, vol. 16, no. 21, pp. 7784–7791, Nov. 2016.

[2] N. Bargshady, G. Garza, and K. Pahlavan, "Precise tracking of things via hybrid 3-D fingerprint database and kernel method particle filter," *IEEE Sensors J.*, vol. 16, no. 24, pp. 8963–8971, Dec. 2016.

[3] H. Zhang, K. Liu, F. Jin, L. Feng, V. Lee, and J. Ng, "A scalable indoor localization algorithm based on distance fitting and fingerprint mapping in Wi-Fi environments," *Neural Comput. Appl.*, vol. 46, pp. 1–15, Jan. 2019.

[4] Y. Zhuang, Y. Li, L. Qi, H. Lan, N. El-Sheimy, and J. Yang, "A two-filter integration of MEMS sensors and WiFi fingerprinting for indoor positioning," *IEEE Sensors J.*, vol. 16, no. 13, pp. 5125–5126, Jul. 2016.

[5] H. Ma and K. Wang, "Fusion of RSS and phase shift using the Kalman filter for RFID tracking," *IEEE Sensors J.*, vol. 17, no. 11, pp. 3551–3558, Jun. 2017.

[6] Y. Duan, W. Nie, K. Liu, Q. Zhuge, H. Edwin, and V. C. Lee, "Joint convergecast and power allocation in wireless sensor networks," in *Proc. 15th Int. Conf. Parallel Distrib. Comput., Appl. Technol.*, Dec. 2014, pp. 98–104.
[7] Q. Jiang, Y. Ma, K. Liu, and Z. Dou, "A probabilistic radio map construction scheme for crowdsourcing-based fingerprinting localization," *IEEE Sensors J.*, vol. 16, no. 10, pp. 3764–3774, May 2016.
[8] W. Zhao, S. Han, R. Q. Hu, W. Meng, and Z. Jia, "Crowdsourcing and multisource fusion-based fingerprint sensing in smartphone localization," *IEEE Sensors J.*, vol. 18, no. 8, pp. 3236–3247, Apr. 2018.
[9] M. Youssef, M. Mah, and A. Agrawala, "Challenges: Device-free passive localization for wireless environments," in *Proc. 13th Annu. ACM Int. Conf. Mobile Comput. Netw.*, Sep. 2007, pp. 222–229.
[10] H. Li, L. Sun, H. Zhu, X. Lu, and X. Cheng, "Achieving privacy preservation in WiFi fingerprint-based localization," in *Proc. INFOCOM*, Apr. 2014, pp. 2337–2345.
[11] Y. Duan, K.-Y. Lam, V. C. Lee, W. Nie, H. Li, and J. K. Ng, "Multiple power path loss fingerprinting for sensor-based indoor localization," *IEEE Sensors Lett.*, vol. 1, no. 4, pp. 1–4, Aug. 2017.
[12] U. M. Qureshi, Z. Umair, Y. Duan, and G. P. Hancke, "Analysis of bluetooth low energy (BLE) based indoor localization system with multiple transmission power levels," in *Proc. IEEE 27th Int. Symp. Ind. Electron. (ISIE)*, Jun. 2018, pp. 1302–1307.
[13] P. Bahl and V. N. Padmanabhan, "Radar: An in-building RF-based user location and tracking system," in *Proc. INFOCOM*, vol. 2, Feb. 2000, pp. 775–784.
[14] X. Liu, J. Cao, S. Tang, J. Wen, and P. Guo, "Contactless respiration monitoring via off-the-shelf WiFi devices," *IEEE Trans. Mobile Comput.*, vol. 15, no. 10, pp. 2466–2479, Oct. 2015.
[15] C. Chen, Y. Chen, Y. Han, H.-Q. Lai, and K. R. Liu, "Achieving centimeter-accuracy indoor localization on WiFi platforms: A frequency hopping approach," *IEEE Internet Things J.*, vol. 4, no. 1, pp. 111–121, Feb. 2017.
[16] K. Liu *et al.*, "Toward low-overhead fingerprint-based indoor localization via transfer learning: Design, implementation, and evaluation," *IEEE Trans. Ind. Inform.*, vol. 14, no. 3, pp. 898–908, Mar. 2018.
[17] K. Kaemarungsi and P. Krishnamurthy, "Properties of indoor received signal strength for WLAN location fingerprinting," in *Proc. 1st Annu. Int. Conf. Mobile Ubiquitous Syst. Netw. Services*, Aug. 2004, pp. 14–23.
[18] C. Feng, W. S. A. Au, S. Valaee, and Z. Tan, "Received-signal-strength-based indoor positioning using compressive sensing," *IEEE Trans. Mobile Comput.*, vol. 11, no. 2, pp. 1983–1993, Dec. 2012.
[19] Z. Chen, H. Zou, H. Jiang, Q. Zhu, Y. C. Soh, and L. Xie, "Fusion of WiFi, smartphone sensors and landmarks using the Kalman filter for indoor localization," *Sensors*, vol. 15, no. 1, pp. 715–732, Jan. 2015.
[20] M. Moussa and M. Youssef, "Smart devices for smart environments: Device-free passive detection in real environments," in *Proc. IEEE Int. Conf. Pervasive Comput. Commun.*, Mar. 2009, pp. 1–6.
[21] J. Gjengset, J. Xiong, G. McPhillips, and K. Jamieson, "Phaser: Enabling phased array signal processing on commodity WiFi access points," in *Proc. 20th Annu. Int. Conf. Mobile Comput. Netw.*, Aug. 2014, pp. 153–164.
[22] G. Deak, K. Curran, and J. Condell, "A survey of active and passive indoor localisation systems," *Comput. Commun.*, vol. 35, no. 16, pp. 1939–1954, Jun. 2012.
[23] *IEEE Trial-Use Recommended Practice for Multi-Vendor Access Point Interoperability Via an Inter-Access Point Protocol Across Distribution Systems Supporting IEEE 802.11 Operation*, IEEE Standard 802.11F-2003, 2003, pp. 1–67.
[24] S. Han, M. Kim, B. Lee, and S. Kang, "Fast directional handoff and lightweight retransmission protocol for enhancing multimedia quality in indoor WLANs," *Comput. Netw.*, vol. 79, pp. 133–147, Aug. 2015.
[25] C.-C. Tseng, K.-H. Chi, M.-D. Hsieh, and H.-H. Chang, "Location-based fast handoff for 802.11 networks," *IEEE Commun. Lett.*, vol. 9, no. 4, pp. 304–306, Apr. 2005.
[26] T. Paul and T. Ogunfrunmiri, "Wireless lan comes of age: Understanding the ieee 802.11 n amendment," *IEEE Circuits Syst. Mag.*, vol. 8, no. 1, pp. 28–54, Jun. 2008.
[27] P. Bahl, V. N. Padmanabhan, and A. Balachandran, "Enhancements to the radar user location and tracking system," Mobility Netw. Res. Group, Microsoft Res., Tech. Rep. MSR-TR-2000-12, Feb. 2000. [Online]. Available: https://www.microsoft.com/en-us/research/publication/enhancements-to-the-radar-user-location-and-tracking-system/
[28] C. E. Palazzi, M. Brunati, and M. Roccetti, "An OpenWRT solution for future wireless homes," in *Proc. IEEE Int. Conf. Multimedia Expo*, Jul. 2010, pp. 1701–1706.
[29] H. Liu, H. Darabi, P. Banerjee, and J. Liu, "Survey of wireless indoor positioning techniques and systems," *IEEE Trans. Syst., Man, Cybern. C, Appl. Rev.*, vol. 37, no. 6, pp. 1067–1080, Nov. 2007.
[30] S. He, T. Hu, and S.-H. G. Chan, "Contour-based trilateration for indoor fingerprinting localization," in *Proc. 13th ACM Conf. Embedded Netw. Sensor Syst.*, May 2015, pp. 225–238.
[31] S. Sorour, Y. Lostanlen, S. Valaee, and K. Majeed, "Joint indoor localization and radio map construction with limited deployment load," *IEEE Trans. Mobile Comput.*, vol. 14, no. 5, pp. 1031–1043, May 2015.

Yaoxin Duan received the B.S. degree from the School of Automatic Control, Huazhong University of Science and Technology, Wuhan, China, in 2006, the M.S. degree from the College of Computer Science, Chongqing University, Chongqing, China, in 2015, and the Ph.D. degree in computer science from the City University of Hong Kong, Hong Kong, in 2018.

From 2018 to 2019, he was a Post-Doctoral Fellow with the City University of Hong Kong. He is currently an Assistant Professor with the College of Automation, Chongqing University of Posts and Telecommunications, Chongqing. His current research interests include Internet of Things, intelligent transportation systems, optimization, wireless networks, and indoor localization.

Kam-Yiu Lam received the B.Sc. (Hons.) degree in computer studies and the Ph.D. degree from the City University of Hong Kong in 1990 and 1994, respectively.

He is currently an Associate Professor with the Department of Computer Science, City University of Hong Kong. His research interests include real-time database systems, real-time active database systems, mobile computing, and distributed multimedia systems.

Victor C. S. Lee received the Ph.D. degree in computer science from the City University of Hong Kong, Hong Kong, in 1997.

He is currently an Assistant Professor with the Department of Computer Science, City University of Hong Kong. His research interests include data dissemination in vehicular networks, real-time databases, and performance evaluation. He is a member of the Association for Computing Machinery (ACM) and the IEEE Computer Society. He was the Chairman of the IEEE Hong Kong Section Computer Chapter from 2006 to 2007.

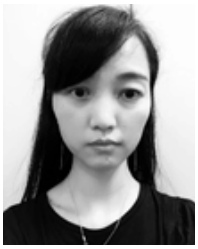

Wendi Nie received the B.E. degree from the School of Automatic Control, Huazhong University of Science and Technology, Wuhan, China, in 2006, the M.S. degree from the College of Computer Science, Chongqing University, Chongqing, China, and the Ph.D. degree in computer science from the City University of Hong Kong, Hong Kong, in 2018.

She is currently an Assistant Professor with the College of Automation, Chongqing University. Her current research interests include big data, intelligent transportation systems, and vehicular networks.

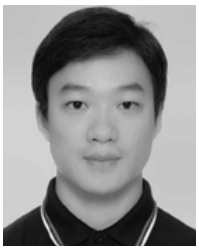

Kai Liu (S'07–M'12) received the Ph.D. degree in computer science from the City University of Hong Kong, Hong Kong, in 2011.

From 2010 to 2011, he was a Visiting Scholar with the Department of Computer Science, University of Virginia, Charlottesville, VA, USA. From 2011 to 2014, he was a Post-Doctoral Fellow with Nanyang Technological University, Singapore, City University of Hong Kong, and Hong Kong Baptist University, Hong Kong. He is currently an Assistant Professor with the College of Computer Science, Chongqing University, Chongqing, China. His research interests include mobile computing, intelligent transportation systems, and vehicular cyber-physical systems.

Hao Li received the B.S. degree from the Department of Computer Science and Engineering, South China University of Technology, Guangzhou, China, in 2016. He is currently pursuing the Ph.D. degree with Hong Kong Baptist University.

His research interests include indoor Wi-Fi positioning and signal processing.

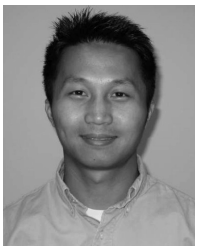

Chun Jason Xue received the B.S. degree in computer science and engineering from The University of Texas at Arlington, Arlington, TX, USA, in 1997, and the M.S. and Ph.D. degrees in computer science from The University of Texas at Dallas, Richardson, TX, USA, in 2002 and 2007, respectively.

He is currently an Associate Professor with the Department of Computer Science, City University of Hong Kong, Hong Kong. His current research interests include memory and parallelism optimization for embedded systems, software/hardware co-design, real-time systems, and computer security.